Inorganic Chemistry

Article

pubs.acs.org/IC

Lanthanide(III) Complexes with Ligands Derived from a Cyclen Framework Containing Pyridinecarboxylate Pendants. The Effect of Steric Hindrance on the Hydration Number

Aurora Rodríguez-Rodríguez,[†] David Esteban-Gómez,[†] Andrés de Blas,[†] Teresa Rodríguez-Blas,[†] Marianna Fekete,[‡] Mauro Botta,[‡] Raphaël Tripier,*[,§] and Carlos Platas-Iglesias*[,†]

[†]Departamento de Química Fundamental, Facultade de Ciencias, Universidade da Coruña, Campus da Zapateira-Rúa da Fraga 10, 15008 A Coruña, Spain

[‡]Dipartimento di Scienze dell' Ambiente e della Vita, Università del Piemonte Orientale "Amedeo Avogadro", Alessandria, Italy

[§]Université de Bretagne Occidentale, UMR-CNRS 6521, UFR des Sciences et Techniques, 6 avenue Victor le Gorgeu, C.S. 93837, 29238 BREST Cedex 3, France

Supporting Information

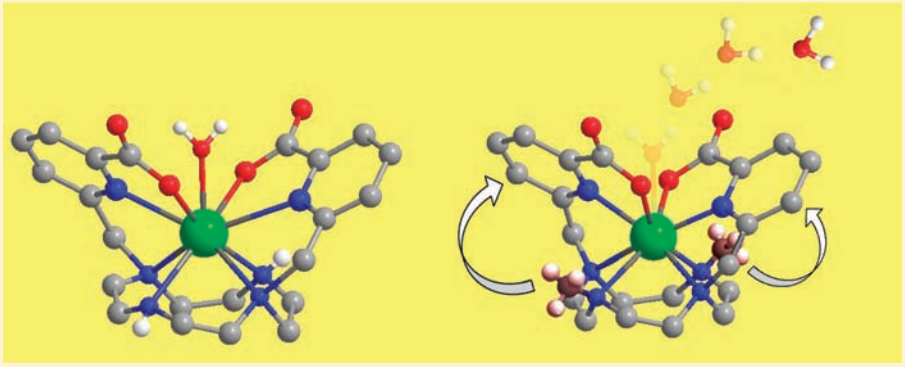

ABSTRACT: Two new macrocyclic ligands, 6,6′-((1,4,7,10-tetraazacyclododecane-1,7-diyl)bis(methylene))dipicolinic acid (H_2DODPA) and 6,6′-((4,10-dimethyl-1,4,7,10-tetraazacyclododecane-1,7-diyl)bis(methylene))dipicolinic acid (H_2Me-DODPA), designed for complexation of lanthanide ions in aqueous solution, have been synthesized and studied. The X-ray crystal structure of [Yb(DODPA)](PF_6)·H_2O shows that the metal ion is directly bound to the eight donor atoms of the ligand, which results in a square-antiprismatic coordination around the metal ion. The hydration numbers (q) obtained from luminescence lifetime measurements in aqueous solution of the Eu^{III} and Tb^{III} complexes indicate that the DODPA complexes contain one inner-sphere water molecule, while those of the methylated analogue H_2Me-DODPA are q = 0. The structure of the complexes in solution has been investigated by ^{1}H and ^{13}C NMR spectroscopy, as well as by theoretical calculations performed at the density functional theory (DFT; mPWB95) level. The minimum energy conformation calculated for the Yb^{III} complex [Λ(λλλλ)] is in good agreement with the experimental structure in solution, as demonstrated by the analysis of the Yb^{III}-induced paramagnetic ^{1}H shifts. The nuclear magnetic relaxation dispersion (NMRD) profiles recorded for [Gd(Me-DODPA)]$^+$ are typical of a complex with q = 0, where the observed relaxivity can be accounted for by the outer-sphere mechanism. However, [Gd(DODPA)]$^+$ shows NMRD profiles consistent with the presence of both inner- and outer-sphere contributions to relaxivity. A simultaneous fitting of the NMRD profiles and variable temperature ^{17}O NMR chemical shifts and transversal relaxation rates provided the parameters governing the relaxivity in [Gd(DODPA)]$^+$. The results show that this system is endowed with a relatively fast water exchange rate k_{ex}^{298} = 58 × 10^6 s^{-1}.

INTRODUCTION

Gadolinium(III) complexes with poly(aminocarboxylate) ligands attract considerable interest because they are commonly used as contrast agents in magnetic resonance imaging (MRI).[1,2] Contrast agents improve the image contrast by preferentially influencing the relaxation efficiency of water proton nuclei in the tissue of interest.[3] A Gd^{III}-based contrast agent for application in MRI should fulfill a number of requirements: (i) the presence of at least one Gd^{III}-bound water molecule that rapidly exchanges with the bulk water of the body, thereby imparting an efficient mechanism for the longitudinal and transverse relaxation enhancement ($1/T_1$ and $1/T_2$) of water protons;[4] (ii) a high thermodynamic and/or kinetic stability under physiological conditions to prevent the release of toxic free Gd^{III} *in vivo*;[5,6] (iii) easy

Received: November 13, 2011
Published: January 13, 2012

   dx.doi.org/10.1021/ic202436j | *Inorg. Chem.* 2012, 51, 2509−2521

functionalization[7] with groups suitable for targeting different tissues, organs or specific biochemical processes at the molecular level in vivo;[8,9] (iv) a high relaxivity,[10] which is a measure of the efficiency of a contrast agent defined as the relaxation-rate enhancement of water protons per mM concentration of metal ion. The relaxation rates of the bulk water around the paramagnetic Gd^{III} ion are enhanced as a result of long-range interactions (outer-sphere relaxivity) and short-range interactions (inner-sphere relaxivity). The latter process depends on a number of parameters that include the rotational correlation time of the complex (τ_R), the residence time of water protons in the innner coordination sphere (τ_m), and the longitudinal and transverse electronic relaxation rates of the metal ion ($1/T_{1e}$ and $1/T_{2e}$). In the past decade an important research effort in this field has been focused on the optimization of these parameters to obtain high relaxivities.[2,10,11]

In recent works we have reported a series of octadentate acyclic ligands containing pyridinecarboxylate units and carboxylate[12] or phosphonate[13−15] pendants designed for stable Ln^{III} complexation in aqueous solutions, their Gd^{III} complexes showing interesting relaxation properties. On the basis of structural considerations, we were able to control the residence time of water protons in the innner coordination sphere, an important parameter to be optimized to obtain efficient MRI contrast agents. More recently we have also reported the macrocyclic ligand H_2BP12C4 (Chart 1),[16] which forms Ln^{III}

Chart 1

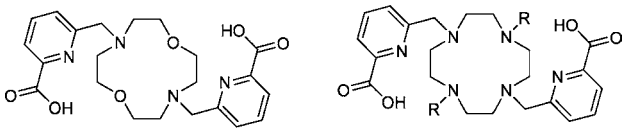

complexes with a reasonably high stability in water.[17] The Gd^{III} complex of $BP12C4^{2-}$ presents an equilibrium in solution between a nona-coordinated species with one inner-sphere water molecule and a ten-coordinated species with two bound water molecules. Interestingly, this complex is also endowed with a very fast water exchange rate.[17]

In the search for innovative structural entries for the design of novel MRI contrast agents, we report here the macrocyclic ligand 6,6′-((1,4,7,10-tetraazacyclododecane-1,7-diyl)bis-(methylene))dipicolinic acid (H_2DODPA, Chart 1). This ligand contains a cyclen unit which, when appropriately modified, represents a very useful platform for the design Ln^{III} complexes with very high thermodynamic and kinetic stabilities.[6] Considering that the most common coordination numbers observed in aqueous solution for Ln^{III} coordination compounds are 8 and 9, at least three and often four of the nitrogen atoms of the cyclen unit must be functionalized with pendant arms to ensure a high stability of the corresponding complexes in water. Indeed, a plethora of works have been carried out to prepare stable cyclen-based Ln^{III} complexes, which often contain carboxylate, methylenephospho(i)nate or acetamide pendant arms.[18] These groups generally contain one donor atom suitable for coordination to the metal ion. Pyridinecarboxylate groups are bidentate coordinating units that are known to provide a strong binding to the Ln^{III} ions.[19,20] Thus, the inclusion of two pyridinecarboxylate groups in positions 1 and 7 of the cyclen framework is expected to provide ligands that (i) ensure a high stability of the corresponding Ln^{III} complexes in water; (ii) provide octadentate binding to the metal ion leaving one coordination position available for an inner-sphere water molecule; (iii) leave two nitrogen atoms of the cyclen unit available for further functionalization with different purposes, that is, conjugation with targeting units, macromolecules, or nanoparticles. As a model for such functionalized derivatives we also report here the ligand 6,6′-((4,10-dimethyl-1,4,7,10-tetraazacyclododecane-1,7-diyl)bis(methylene))dipicolinic acid (H_2Me-DODPA, Chart 1), which contains methyl groups at positions 4 and 10 of the cyclen backbone. The lanthanide complexes of DODPA and Me-DODPA were characterized by ^{1}H and ^{13}C NMR techniques in D_2O solution. Luminescence lifetime measurements on the Eu^{III} and Tb^{III} complexes have been carried out to determine the hydration number of the complexes in solution. In addition, the complexes were characterized by density functional theory (DFT) calculations, and the structure established by these calculations was compared with the structural information obtained in solution from paramagnetic NMR measurements (Yb^{III}-induced ^{1}H NMR shifts). Finally, nuclear magnetic relaxation dispersion (NMRD) investigations and variable-temperature ^{17}O NMR measurements of the Gd^{III} complexes were performed to assess their ^{1}H relaxation enhancement abilities and to gain insight into the parameters governing the relaxivity.

EXPERIMENTAL SECTION

General Methods. Elemental analyses were carried out on a Carlo Erba 1108 elemental analyzer. ESI-TOF mass spectra were recorded using a LC-Q-q-TOF Applied Biosystems QSTAR Elite spectrometer in the positive mode. IR-spectra were recorded using a Bruker Vector 22 spectrophotometer equipped with a Golden Gate Attenuated Total Reflectance (ATR) accessory (Specac). ^{1}H and ^{13}C NMR spectra were recorded at 25 °C on Bruker Avance 300 and Bruker Avance 500 MHz spectrometers. For measurements in D_2O, *tert*-butyl alcohol was used as an internal standard with the methyl signal calibrated at δ = 1.2 (^{1}H) and 31.2 ppm (^{13}C). Spectral assignments were based in part on two-dimensional COSY, EXSY, HSQC, and HMBC experiments. UV−vis spectra were recorded on a Perkin-Elmer Lambda 900 spectrophotometer in 1.0 cm path quartz cells. Excitation and emission spectra were recorded on a Perkin-Elmer LS-50B spectrometer. Luminescence lifetimes were calculated from the monoexponential fitting of the average decay data, and they are averages of at least 3−5 independent determinations.

NMRD and ^{17}O NMR Measurements. The water proton longitudinal relaxation rates as a function of temperature (20 MHz) were measured with a Stelar Spinmaster Spectrometer FFC−2000 (Mede, Pv, Italy) on about 0.8−1.9 mM aqueous solutions in nondeuterated water. The exact concentrations of gadolinium were determined by measurement of bulk magnetic suceptibility shifts of a *t*BuOH signal on a Bruker Avance III spectrometer (11.7 T).[21] The ^{1}H T_1 relaxation times were acquired by the standard inversion recovery method with typical 90° pulse width of 3.5 μs, 16 experiments of 4 scans. The reproducibility of the T_1 data was ±5%. The temperature was controlled with a Stelar VTC-91 airflow heater equipped with a calibrated copper−constantan thermocouple (uncertainty of ±0.1 °C). The proton $1/T_1$ NMRD profiles were measured on a fast field-cycling Stelar SmartTracer relaxometer over a continuum of magnetic field strengths from 0.00024 to 0.25 T (corresponding to 0.01−10 MHz proton Larmor frequencies). The relaxometer operates under computer control with an absolute uncertainty in $1/T_1$ of ±1%. Additional data points in the range 15−70 MHz were obtained on a

dx.doi.org/10.1021/ic202436j | Inorg. Chem. 2012, 51, 2509−2521

Bruker WP80 NMR electromagnet adapted to variable-field measurements (15−80 MHz proton Larmor frequency) Stelar Relaxometer.

Variable-temperature ^{17}O NMR measurements were recorded on a Bruker Avance III (11.7 T) spectrometer equipped with a 5 mm probe and standard temperature control units. Aqueous solutions of the complex (16 mM) containing 2.0% of the ^{17}O isotope (Cambridge Isotope) were used. The observed transverse relaxation rates were calculated from the signal width at half-height. The bulk magnetic suceptibility contribution was subtracted from the ^{17}O NMR shift data using the ^{1}H NMR shifts of the $^{t}BuOH$ signal as internal reference.

Single Crystal X-ray Diffraction Measurements. Three dimensional X-ray data were collected on a Bruker-Nonius X8 APEX Kappa CCD diffractometer. Data were corrected for Lorentz and polarization effects and for absorption by semiempirical methods[22] based on symmetry-equivalent reflections. Complex scattering factors were taken from the program SHELX97[23] running under the WinGX program system[24] as implemented on a Pentium computer. The structure was solved by Patterson methods with DIRDIF2008[25] and refined[23] by full-matrix least-squares on F^2. The hydrogen atoms were included in calculated positions and refined in riding mode, except those of the water molecule that were located in a difference electron-density map and all the parameters fixed. The noncoordinated PF_6^- anion shows positional disorder with occupational factors of 0.738(6) for F atoms labeled with A. The refinement converged with anisotropic displacement parameters for all non-hydrogen atoms. Crystal data and details on data collection and refinement are summarized in Table 1.

Table 1. Crystal Data and Refinement Details for $[Yb(DODPA)](PF_6)\cdot H_2O$

formula	$C_{22}H_{30}F_6N_6O_5PYb$	λ, Å (MoK$_\alpha$)	0.71073
MW	776.53	D_{calc}/g cm^{-3}	1.981
crystal system	monoclinic	μ/mm^{-1}	3.744
space group	$P2_1/c$	θ range/deg	2.00 to 28.37
T/K	100(2)	R_{int}	0.0316
a/Å	9.5249(3)	reflns measd	57955
b/Å	13.4108(5)	unique reflns	6479
c/Å	20.5030(7)	reflns obsd	6094
β/deg	96.225(2)	GOF on F^2	1.249
V/Å^3	2603.54(16)	R_1[a]	0.0324
F(000)	1532	wR_2 (all data)[b]	0.0822
Z	4	largest differences peak and hole/e Å^{-3}	2.907 and −1.104

[a] $R_1 = \sum||F_o| - |F_c||/\sum|F_o|$. [b] $wR_2 = \{\sum w(F_o^2 - F_c^2)^2/\sum w(F_o^4)\}^{1/2}$.

Chemicals and Starting Materials. 1,7-Bis(*tert*-butyloxycarbonyl)-tetraazacyclododecane (**1**),[26] 6-chloromethylpyridine-2-carboxylic acid methyl ester (**2**),[16] and cyclen glyoxal (**4**)[27] were prepared according to the literature methods. All other chemicals were purchased from commercial sources and used without further purification, unless otherwise stated. Silica gel (Fluka 60, 0.063−0.2 mm) was used for preparative column chromatography.

Dimethyl 6,6′-((4,10-*tert*-butyloxycarbonyl-1,4,7,10-tetraazacyclododecane-1,7-diyl)bis(methylene))dipicolinate (3). A mixture of 1,7-bis(*tert*-butyloxycarbonyl)-tetraazacyclododecane (**1**) (1.287 g, 3.46 mmol), Na_2CO_3 (1.831 g, 17.30 mmol) in acetonitrile (150 mL) was heated to reflux for 5 min, and then compound **2** (see Scheme 1, 1.283 g, 6.91 mmol) dissolved in acetonitrile (3 mL) was added. The mixture was heated to reflux with stirring for a period of 48 h, and then the excess of Na_2CO_3 was filtered off. The filtrate was concentrated to dryness and the yellow residue partitioned between equal volumes (50 mL) of H_2O and $CHCl_3$. The aqueous phase was extracted with $CHCl_3$ (4 × 50 mL), and the combined organic extracts were dried over $NaSO_4$, filtered, and evaporated to dryness. The crude product was purified by using column chromatography (SiO_2, $CHCl_3$ to 10% MeOH in $CHCl_3$) to yield 2.115 g of the desired compound as a yellow oil (91%). Anal. Calcd. for $C_{34}H_{50}N_6O_8\cdot 0.5CHCl_3$: C, 56.73; H, 6.97; N, 11.50%. Found: C, 56.71; H, 7.10; N, 11.36%. δ_H (solvent CD_3SOCD_3, 295 K, 300 MHz): 7.91 (m, 4H, py); 7.65 (m, 2H, py); 3.10−3.50 (b, 8H, $-CH_2-$); 2.50−2.70 (b, 6H, $-CH_2-$); 3.87 (s, 6H, $-OCH_3$); 3.76 (s, 4H, $-CH_2-$) 1.17 (s, 18H, ^{t}Bu). IR: 1723 and 1682 ν(C=O), 1589 $\nu(C{=}N)_{py}$ cm^{-1}. MS (ESI$^+$): m/z 693 ($[C_{34}H_{50}N_6NaO_8]^+$).

6,6′-((1,4,7,10-Tetraazacyclododecane-1,7-diyl)bis-(methylene))dipicolinic Acid (H_2DODPA). A solution of compound **3** (0.804 g, 1.20 mmol) in 6 M HCl (10 mL) was heated to reflux for 24 h. The solution was concentrated to dryness, and the resulting yellow oil was dissolved in MeOH (5 mL) and the solvent evaporated. This procedure was repeated twice, and another three times with diethyl ether (3 × 5 mL) to yield 0.709 g of the desired compound as a pale yellow foam (85%). Anal. Calcd. for $C_{22}H_{30}N_6O_4\cdot 5HCl\cdot 4H_2O$: C, 37.92; H, 6.22; N, 12.06%. Found: C, 37.75; H, 6.28; N, 12.04%. δ_H (solvent D_2O, 295 K, 500 MHz, pD = 0.7): 7.75 (m, 2H, py); 7.59 (d, 2H, py, ^3J = 7.6 Hz); 7.37 (d, 2H, py, ^3J = 7.8 Hz); 4.05 (s, 4H, $-CH_2-$); 3.37 (b, 4H, $-CH_2-$); 3.27 (b, 4H, $-CH_2-$); 3.11 (b, 4H, $-CH_2-$); 2.90 (b, 4H, $-CH_2-$). δ_C (solvent D_2O, 295 K, 125.8 MHz, pD = 0.7): 42.6, 48.8, 55.2 (secondary C); 123.9, 126.3, 137.6 (tertiary C); 145.3, 158.4, 167.0 (quaternary C). IR: 1692 ν(C=O), 1462 $\nu(C{=}N)_{py}$ cm^{-1}. MS (ESI$^+$): m/z 443 ($[C_{22}H_{31}N_6O_4]^+$), 222 ($[C_{22}H_{32}N_6O_4]^{2+}$).

Compound 5. This compound was prepared by using a slight modification of the literature procedure.[28] Compound **4** (1.551 g, 7.98 mmol) was dissolved in dry CH_3CN (18 mL), and a solution of MeI (1095 μL, 17.56 mmol) in the same solvent (10 mL) was added dropwise over a period of 4 h. The mixture was stirred at room temperature for 72 h. The white precipitate formed was isolated by filtration and washed with CH_3CN (3× 5 mL) and diethyl ether (3 × 5 mL), and dried under vacuum to give 3.403 g of **5** (89%) as a white solid. Anal. Calcd. for $C_{12}H_{24}I_2N_4$: C, 30.14; H, 5.06; N, 11.72%. Found: C, 30.15; H, 4.98; N, 11.55%. δ_H (solvent D_2O, 295 K, 300 MHz): 4.53 (s, 4H, −CH−); 4.20−3.85 (m, 8H, $-CH_2-$); 3.75−3.55 (m, 4H, $-CH_2-$); 3.44 (s, 6H, $-CH_3$); 3.30−3.05 (m, 4H, $-CH_2-$). δ_C (solvent D_2O, 295 K, 75.5 MHz): 46.5 (primary C); 43.0, 46.7, 59.1, 65.0 (secondary C); 78.1 (tertiary C). MS (ESI$^+$): m/z 351 ($[C_{12}H_{24}IN_4]^+$), 112 ($[C_{12}H_{24}N_4]^{2+}$).

1,7-Dimethyl-1,4,7,10-tetraazacyclododecane (6). Compound **5** (2.929 g, 6.13 mmol) was dissolved in hydrazine monohydrate (15 mL) and the mixture heated to reflux over a period of 4 h. The solution was allowed to cool down to room temperature and then stored at 5 °C for 4 h. The white crystals formed were collected by filtration and washed with cold hydrazine monohydrate (2 mL). The solid was dissolved in EtOH (20 mL), and the solvent removed in a rotary evaporator. This process was repeated five times, resulting in the formation of an oily residue. Addition of diethyl ether (40 mL) and subsequent evaporation of the solvent gave 0.980 g of the desired compound as a pale-brown oil (80%). δ_H (solvent $CDCl_3$, 295 K, 300 MHz): 2.70 (m, 8H, $-CH_2-$); 2.53 (m, 8H, py, $-CH_2-$); 2.32 (s, 6H, $-CH_3$). δ_C (solvent $CDCl_3$, 295 K, 75.5 MHz): 44.4 (primary C); 45.5, 54.3 (secondary C). MS (ESI$^+$): m/z 201 ($[C_{10}H_{25}N_4]^+$).

Dimethyl 6,6′-((4,10-dimethyl-1,4,7,10-tetraazacyclododecane-1,7-diyl)bis(methylene))dipicolinate (7). Compound **6** (0.980 g, 4.89 mmol) was dissolved in dry CH_3CN (40 mL), and K_2CO_3 (2.703 g, 19.56 mmol) was added. A solution of 6-chloromethylpyridine-2-carboxylic acid methyl ester (**2**) in the same solvent (20 mL) was added dropwise to the former solution over a period of 6 h. The mixture was stirred at room temperature for 6 days, and then at 40 °C for 3 days. The excess of K_2CO_3 was filtered off, and the filtrate concentrated to dryness. The oily residue was partitioned between H_2O (20 mL) and $CHCl_3$ (50 mL). The organic phase was collected and the aqueous phase extracted with $CHCl_3$ (2 × 40 mL). The combined organic extracts were dried over $MgSO_4$, and the solvent was evaporated to give a brown oil. This was purified by using column chromatography (neutral Al_2O_3, $CHCl_3$ to 6% MeOH in $CHCl_3$) to yield 1.097 g of the desired compound as a yellow oil (45%). δ_H (solvent $CDCl_3$, 295 K, 300 MHz): 7.73 (d, 2H, py); 7.62 (d, 2H, py); 7.57 (m, 2H, py); 3.70 (s, 4H, $-CH_2-$); 3.60 (s, 6H, $-CH_3$); 2.44 (s, 16H, $-CH_2-$); 2.33 (s, 6H, $-CH_3$). δ_C (solvent

dx.doi.org/10.1021/ic202436j | Inorg. Chem. 2012, 51, 2509−2521

Scheme 1

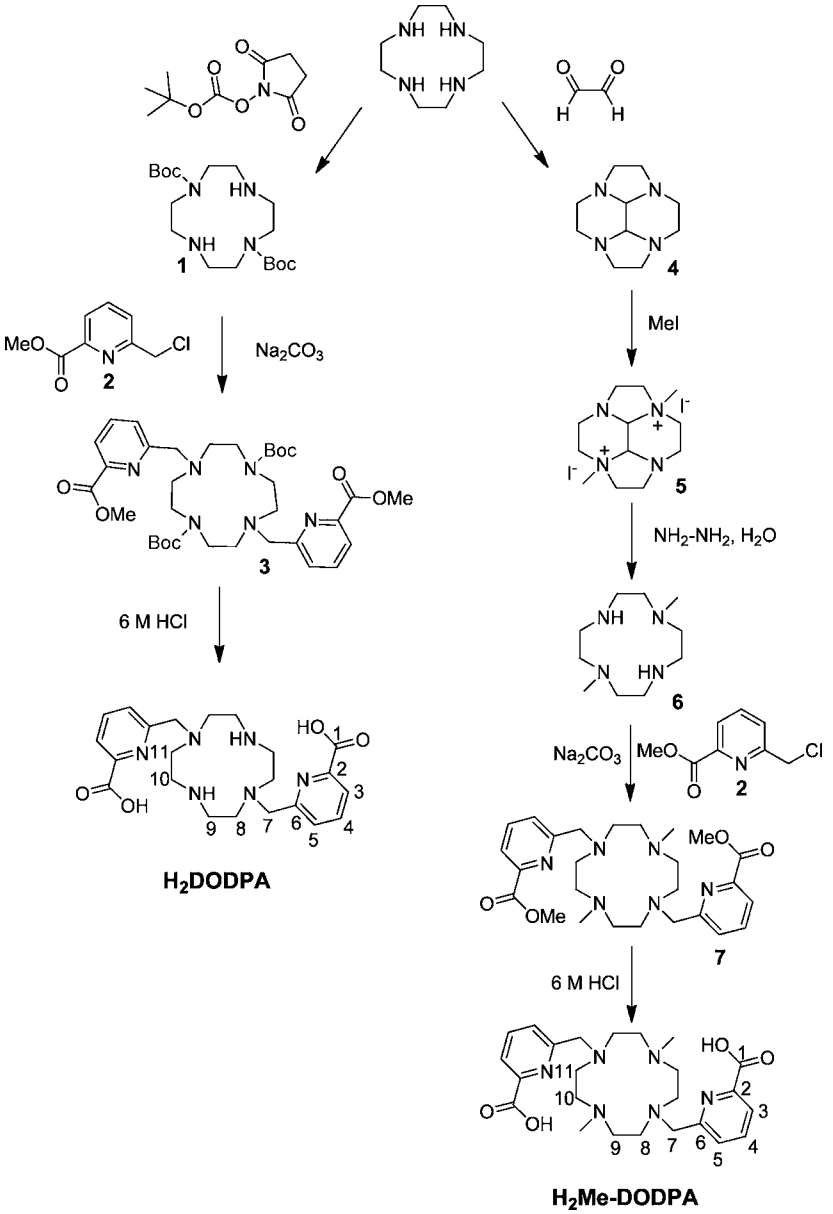

$CDCl_3$, 295 K, 75.5 MHz): 43.2, 55.5 (primary C); 52.2, 61.2 (secondary C); 122.8, 125.9, 134.0 (tertiary C); 146.6, 161.1, 165.2 (quaternary C). IR: 1716 ν(C═O), 1589 $\nu(C{=}N)_{py}$ cm^{-1}. MS (ESI^+): m/z 499 ($[C_{26}H_{39}N_6O_4]^+$), 521 ($[C_{26}H_{38}N_6NaO_4]^+$).

6,6′-((4,10-Dimethyl-1,4,7,10-tetraazacyclododecane-1,7-diyl)bis(methylene))dipicolinic acid (H_2Me-DODPA). A solution of compound **7** (0.795 g, 1.59 mmol) in 6 M HCl (70 mL) was heated to reflux for 12 h. The solution was concentrated to dryness to give 1.00 g of the desired compound as a pale-yellow crystalline solid (85%). Anal. Calcd. for $C_{24}H_{34}N_6O_4{\cdot}7HCl{\cdot}H_2O$: C, 38.75; H, 5.83; N, 11.30%. Found: C, 38.72; H, 6.05; N, 11.09%. δ_H (solvent D_2O, 295 K, 300 MHz, pD = 0.7): 7.91 (m, 2H, py); 7.82 (d, 2H, py, ^3J = 7.5 Hz); 7.56 (d, 2H, py, ^3J = 7.8 Hz); 4.17 (s, 4H, $-CH_2-$); 3.55 (b, 4H, $-CH_2-$); 3.37 (b, 4H, $-CH_2-$); 3.18 (b, 4H, $-CH_2-$); 2.99 (b, 4H, $-CH_2-$); 2.74 (s, 6H, $-CH_3$). δ_C (solvent D_2O, 295 K, 125.8 MHz, pD = 0.7): 43.3, (primary C); 49.1, 53.1, 56.2 (secondary C); 124.5, 127.2, 138.5 (tertiary C); 145.4, 158.7, 166.3 (quaternary C). IR: 1730 ν(C═O), 1615 $\nu(C{=}N)_{py}$ cm^{-1}. MS (ESI^+): m/z 236 ($[C_{24}H_{36}N_6O_4]^{2+}$), 471 ($[C_{24}H_{35}N_6O_4]^+$).

General Procedure for the Preparation of [Ln(DODPA)]Cl Complex Salts. A solution of H_2DODPA·4HCl·H_2O (0.100 g, 0.160 mmol) and triethylamine (172 μL, 1.23 mmol) in methanol (7 mL) was heated to reflux. Then, a solution of $LnCl_3{\cdot}6H_2O$ (0.160 mmol, Ln = La, Eu, Gd, Tb, Yb, or Lu) in methanol (3 mL) was slowly added drop by drop. The mixture was heated to reflux for 72 h. After that, the reaction mixture was allowed to cool to room temperature and then concentrated to dryness. The addition of CH_3CN (4 mL) resulted in the formation of a white precipitate. The mixture was stirred at room temperature for 24 h, and then the solid was isolated by filtration, washed with CH_3CN (3 × 4 mL) and diethyl ether (3 × 4 mL), and dried under vacuum.

[La(DODPA)]Cl. Yield 0.023 g, 25%. HS-MS (ESI^+): m/z 579.1226; calcd. for $[C_{22}H_{28}LaN_6O_4]^+$ 579.1236. IR (ATR, cm^{-1}): ν 1628 (C═O), ν 1583 $(C{=}N)_{py}$.

[Eu(DODPA)]Cl. Yield 0.061 g, 65%. HS-MS (ESI^+): m/z 593.1371; calcd. for $[C_{22}H_{28}EuN_6O_4]^+$ 593.1384. IR (ATR, cm^{-1}): ν 1632 (C═O), ν 1588 $(C{=}N)_{py}$.

[Gd(DODPA)]Cl. Yield 0.049 g, 46%. HS-MS (ESI^+): m/z 598.1412; calcd. for $[C_{22}H_{28}LGdN_6O_4]^+$ 598.1413. IR (ATR, cm^{-1}): ν 1714 (C═O), ν 1585 $(C{=}N)_{py}$.

dx.doi.org/10.1021/ic202436j | Inorg. Chem. 2012, 51, 2509−2521

[Tb(DODPA)]Cl. Yield 0.066 g, 70%. HS-MS (ESI$^+$): m/z 599.1420; calcd. for $[C_{22}H_{28}N_6O_4Tb]^+$ 599.1425. IR (ATR, cm^{-1}): ν 1653(C=O), ν 1593 $(C{=}N)_{py}$.

[Yb(DODPA)]Cl. Yield 0.066 g, 68%. HS-MS (ESI$^+$): m/z 614.1564; calcd. for $[C_{22}H_{28}N_6O_4Yb]^+$ 614.1561. IR (ATR, cm^{-1}): ν 1646 (C=O), ν 1597 $(C{=}N)_{py}$.

[Lu(DODPA)]Cl. Yield 0.063 g, 65%. HS-MS (ESI$^+$): m/z 615.1576; calcd. for $[C_{22}H_{28}LuN_6O_4]^+$ 615.1580. IR (ATR, cm^{-1}): ν 1633 (C=O), ν 1595 $(C{=}N)_{py}$.

General Procedure for the Preparation of [Ln(Me-DODPA)]Cl Complex Salts. The same procedure used for the H_2DODPA analogues was followed by using of H_2Me-DODPA·7HCl·H_2O (0.100 g, 0.130 mmol), thiethylamine (197 μL, 1.41 mmol) and $LnCl_3$·$6H_2O$ (0.130 mmol, Ln = La, Eu, Gd, Tb, Yb, or Lu) in methanol (10 mL).

[La(Me-DODPA)]Cl. Yield 0.078 g, 89%. HS-MS (ESI$^+$): m/z 607.1535; calcd. for $[C_{24}H_{32}LaN_6O_4]^+$ 607.1549. IR (ATR, cm^{-1}): ν 1624 (C=O), ν 1588 $(C{=}N)_{py}$.

[Eu(Me-DODPA)]Cl. Yield 0.074 g, 84%. HS-MS (ESI$^+$): m/z 621.1696; calcd. for $[C_{24}H_{32}EuN_6O_4]^+$ 621.1697. IR (ATR, cm^{-1}): ν 1658 (C=O), ν 1600 $(C{=}N)_{py}$.

[Gd(Me-DODPA)]Cl. Yield 0.076 g, 85%. HS-MS (ESI$^+$): m/z 626.1724; calcd. for $[C_{24}H_{32}GdN_6O_4]^+$ 626.1726. IR (ATR, cm^{-1}): ν 1657 (C=O), ν 1600 $(C{=}N)_{py}$.

[Tb(Me-DODPA)]Cl. Yield 0.086 g, 95%. HS-MS (ESI$^+$): m/z 627.1732; calcd. for $[C_{24}H_{32}N_6O_4Tb]^+$ 627.1738. IR (ATR, cm^{-1}): ν 1659 (C=O), ν 1601 $(C{=}N)_{py}$.

[Yb(Me-DODPA)]Cl. Yield 0.082 g, 90%. HS-MS (ESI$^+$): m/z 642.1872; calcd. for $[C_{24}H_{32}N_6O_4Yb]^+$ 642.1874. IR (ATR, cm^{-1}): ν 1660 (C=O), ν 1602 $(C{=}N)_{py}$.

[Lu(Me-DODPA)]Cl. Yield 0.069 g, 76%. HS-MS (ESI$^+$): m/z 643.1871; calcd. for $[C_{24}H_{32}LuN_6O_4]^+$ 643.1893. IR (ATR, cm^{-1}): ν 1660 (C=O), ν 1602 $(C{=}N)_{py}$.

Computational Methods. All calculations were performed employing DFT within the meta generalized gradient approximation (meta-GGA), with the mPWB95 exchange-correlation functional,[29,30] and the Gaussian 09 package (Revision A.02).[31] On the grounds of our previous experience, full geometry optimizations of the $[Ln(DODPA)(H_2O)_q]^+$ and $[Ln(Me\text{-}DODPA)(H_2O)_q]^+$ (Ln = La, Nd, Eu, Gd, Ho, Yb, or Lu; q = 0 or 1) systems were performed in water solution by using the effective core potential (ECP) of Dolg et al. and the related [5s4p3d]-GTO valence basis set for the lanthanides,[32] and the 6-31G(d) basis set for C, H, N, and O atoms. No symmetry constraints have been imposed during the optimizations. The default values for the integration grid ("fine") and the SCF energy convergence criteria (10^{-8}) were used. The stationary points found on the potential energy surfaces as a result of the geometry optimizations have been tested to represent energy minima rather than saddle points via frequency analysis. Solvent effects were evaluated by using the polarizable continuum model (PCM), in which the solute cavity is built as an envelope of spheres centered on atoms or atomic groups with appropriate radii. In particular, we used the integral equation formalism (IEFPCM) variant as implemented in Gaussian 09.[33] In aqueous solution relative free energies of the different isomers include nonpotential-energy contributions (zero point energies and thermal terms) obtained through frequency analysis.

RESULTS AND DISCUSSION

Synthesis of the Ligands and Lanthanide Complexes. The synthetic protocols used for the preparation of H_2DODPA and H_2Me-DODPA are shown in Scheme 1. The synthesis of H_2DODPA involved the preparation of diBoc-cyclen (**1**) following the previous reported reaction of cyclen with *tert*-butyl-(oxycarbonyloxy)succinimide.[26] Alkylation of **1** with the 6-chloromethylpyridine derivative **2**[16] in refluxing acetonitrile in the presence of Na_2CO_3 gave compound **3** in 91% yield. Full deprotection of the methyl esters of **3** and the *tert*-butyl carbamate groups was cleanly achieved with 6 M HCl to yield the desired ligand H_2DODPA with an overall yield of 77% as calculated from cyclen. The synthesis of H_2Me-DODPA was achieved by using the now well-known bis-aminal chemistry.[34] Cyclen glyoxal (**1**) was quantitatively obtained by direct condensation of glyoxal with cyclen,[27] the subsequent *trans*-alkylation with iodomethane leading to compound **5** in 89% yield. The reductive cleavage of **5** with hydrazine monohydrate gave compound **6** in good yield (80%).[27] Alkylation of **6** with the 6-chloromethylpyridine derivative **2**, as previously described for **1**, followed by deprotection of the methyl ester groups with 6 M HCl gave the desired ligand in 27% yield as calculated from cyclen. Reaction of ligands H_2DODPA or H_2Me-DODPA with hydrated lanthanide chlorides in the presence of an excess of triethylamine resulted in the formation of compounds of formula [Ln(L)]Cl (L = DODPA or Me-DODPA; Ln = La, Eu, Gd, Tb, Yb, or Lu). Compounds [Ln(Me-DODPA)]Cl were isolated in 76–95% yields, while the [Ln(DODPA)]Cl yields were somewhat lower (25–70%). The high resolution mass spectra (ESI$^+$-MS) show peaks due to the $[Ln(L)]^+$ entities, thereby confirming the formation of the desired compounds.

X-ray Crystal Structure of [Yb(DODPA)](PF$_6$)·H$_2$O. Addition of an excess of KPF_6 to an aqueous solution of the $[Yb(DODPA)]^+$ complex resulted in the formation of single crystals suitable for X-ray diffraction analysis. Crystals contain the cation $[Yb(DODPA)]^+$, one heavily disordered hexafluorophosphate anion, and a noncoordinating water molecule. Figure 1 shows a view of the complex cation, while bond

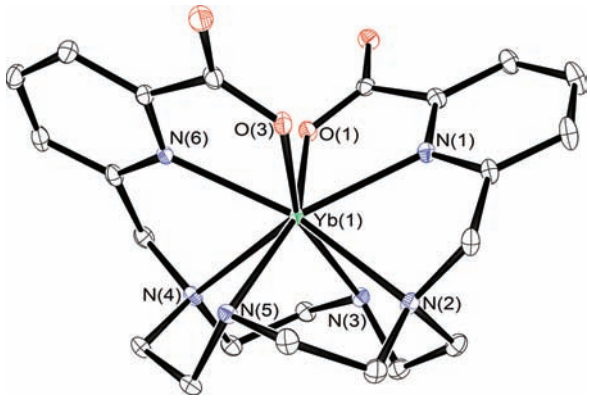

Figure 1. X-ray crystal structure of the cation $[Yb(DODPA)]^+$ with atom labeling; hydrogen atoms are omitted for simplicity. The ORTEP plot is drawn at the 30% probability level.

distances of the metal coordination environment are given in Table 2. The metal ion is directly bound to the eight donor

Table 2. Selected Bond Lengths (Å) of the Metal Coordination Environment in [Yb(DODPA)](PF$_6$)·H$_2$O[a]

Yb(1)–O(1)	2.242(3)	Yb(1)–N(5)	2.429(3)
Yb(1)–O(3)	2.247(3)	Yb(1)–N(3)	2.430(3)
Yb(1)–N(1)	2.359(3)	Yb(1)–N(2)	2.520(3)
Yb(1)–N(6)	2.368(3)	Yb(1)–N(4)	2.535(3)

[a]See Figure 1 for labeling.

atoms of the ligand, which adopts a *syn* conformation with the two pendant arms disposed on the same side of the macrocyclic unit. The distances between the Yb^{III} ion and the pivotal nitrogen atoms [N(2) and N(4)] are about 0.1 Å longer than the Yb(1)–N(5) and Yb(1)–N(3) distances. The distances between the Ln^{III} ion and the nitrogen atoms of the cyclen

dx.doi.org/10.1021/ic202436j | Inorg. Chem. 2012, 51, 2509–2521

moiety are about 0.08−0.18 Å shorter than those observed[35] for [Lu(DOTA)]$^-$, pointing to a rather strong binding of the cyclen unit to the metal ion in [Yb(DODPA)]$^+$. The distances between the lanthanide and the donor atoms of the picolinate pendants are about 0.03−0.09 Å shorter than those found for an eight-coordinate Lu^{III} complex containing picolinate moieties.[36] The [Yb(DODPA)]$^+$ cation shows a slightly distorted C_2 symmetry in the solid state, where the symmetry axis is perpendicular to the pseudoplane described by the four donor atoms of the crown moiety and contains the Yb^{III} ion.

The coordination polyhedron around the Yb^{III} ion can be described as a severely distorted twisted-square antiprism composed of two parallel pseudo planes: O(1), O(3), N(1), and N(6) define the upper pseudo plane (mean deviation from planarity 0.211 Å), while N(2), N(3), N(4), and N(5) define the lower pseudo plane (mean deviation from planarity 0.046 Å). The angle between these two least-squares planes amounts to 0.7°, and the Yb^{III} ion is placed at 1.23 Å from the upper plane and 1.41 Å from the plane defined by the nitrogen atoms of the cyclen unit. As described in detail for [Ln(DOTA)]$^-$ complexes,[37] the *syn* conformation of the ligand in the [Yb(DODPA)]$^+$ complex implies the occurrence of two helicities (one belonging to the crown moiety and one associated with the layout of the pendant arms).[38,39] Inspection of the crystal structure data reveals that two $\Delta(\delta\delta\delta\delta)$ and $\Lambda(\lambda\lambda\lambda\lambda)$ enantiomers cocrystallize in equal amounts (racemate). The mean twist angle, ω,[40] between these nearly parallel squares is −30.5°, in line with a twisted-square antiprismatic (TSAP) coordination polyhedron around the metal ion. This twist angle is somewhat larger than that observed for the TSAP isomer of [Tm(DOTA)]$^-$ (−24.5°).[41]

Assessment of the Hydration State. A desirable optical property of the Ln^{III} complexes of DODPA and Me-DODPA is the presence of picolinate moieties that can act as an antenna to sensitize the emission of Eu^{III} and Tb^{III}. Indeed, the absorption spectra of the Eu^{III} and Tb^{III} complexes show a band with a maximum at about 272 nm that can be assigned to a combination of $\pi\rightarrow\pi^*$ and $n\rightarrow\pi^*$ transitions centered on the picolinate moieties (Figure 2).[42] The emission spectra of about

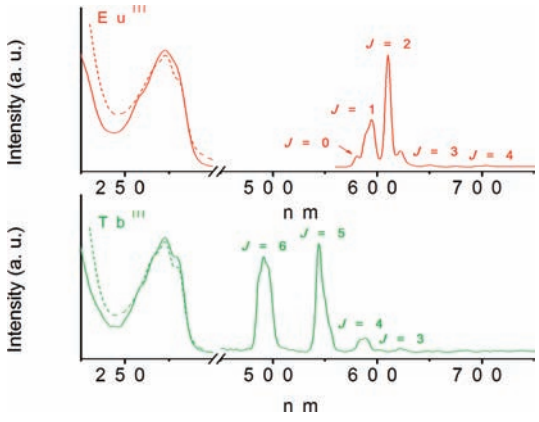

Figure 2. Absorption (dotted lines), excitation and emission spectra of the Eu^{III} and Tb^{III} complexes of Me-DODPA as recorded in H_2O solution (10^{-5} M, pH ~ 7.0) at room temperature.

10^{-5} M solutions of the Eu^{III} and Tb^{III} complexes of in H_2O (pH ~ 7.0 and 295 K), obtained under excitation through the ligand bands at 272 nm, display the $^5D_0 \rightarrow {}^7F_J$ (Eu^{III}, J = 0−4) or $^5D_4 \rightarrow {}^7F_J$ (Tb^{III}, J = 6−3) transitions characteristic of the particular Ln^{III} ion (Figure 2). The excitation spectra recorded upon metal centered emission are very similar to the corresponding absorption spectra, indicating that the coordinated picolinate moieties provide an efficient energy transfer to the Eu^{III} and Tb^{III} ions.

The emission lifetimes of the Eu($^5D_0$) and Tb($^5D_4$) excited levels have been measured in D_2O and H_2O solutions of the complexes, and were used to calculate the number of coordinated water molecules q (Table 3). The luminescence

Table 3. Lifetimes of the of Eu($^5D_0$) and Tb($^5D_4$) Excited States in DODPA and Me-DODPA Complexes and Hydration Numbers (q)

Ln	τ_{H_2O}/ms	τ_{D_2O}/ms	q^a
[Eu(DODPA)]$^+$	0.26	0.39	1.1
[Eu(Me-DODPA)]$^+$	0.91	1.27	0.0
[Tb(DODPA)]$^+$	1.18	1.51	0.6
[Tb(Me-DODPA)]$^+$	2.39	2.68	0.0

$^a\Delta k_{obs} = k_{obs}(H_2O) - k_{obs}(D_2O)$ and $k_{obs} = 1/\tau_{obs}$. $q_{Eu} = 1.11(\Delta k_{obs} - 0.31)$;[43] $q_{Tb} = 5.0(\Delta k_{obs} - 0.06)$.[44]

lifetimes determined for the DODPA complexes are clearly shorter than those obtained for the Me-DODPA derivatives. This is in agreement with a higher hydration number and an important quenching effect of the ligand NH oscillators in DODPA complexes. As pointed out by ^{1}H NMR measurements (see below) the exchange between the ligand NH protons and deuterium in D_2O is very slow. However, the emission lifetimes recorded in D_2O solution were progressively increasing with the passing of time as a consequence of the exchange between NH protons of the ligand and the solvent, and therefore the τ_{D_2O} values used for hydration number calculations were measured from freshly prepared solutions of the complexes. The results obtained for the DODPA complexes are consistent with the presence of one-inner-sphere water molecule, the average hydration number obtained for the Eu^{III} and Tb^{III} complexes amounting to 0.8. In contrast, the luminescence lifetimes determined for Me-DODPA complexes point to a hydration number of zero, in line with the coordination sphere saturated by the eight heteroatoms of the ligand (4 N atoms from the cyclen moiety, 2 O atoms from the carboxylate functions, and 2 N atoms of the pyridyl rings). These results suggest that the introduction of two methyl groups in DODPA causes a certain degree of steric hindrance that precludes the coordination of water molecules to the metal ion. The hydration numbers obtained for [Ln(DODPA)]$^+$ complexes (Ln = Eu, Tb) are lower than those previously determined for [Eu(BP12C4)]$^+$.[16] For the latter complex UV−vis measurements revealed the presence of an equilibrium in solution involving a ten-coordinated species with q = 2 and a nine-coordinated species with q = 1, the average hydration number at 298 K amounting to q = 1.4.

Structure of the Complexes in Solution. The ^{1}H and ^{13}C NMR spectra of the diamagnetic Lu^{III} complex of DODPA and Me-DODPA were obtained in D_2O solution at pD = 7.0 and 298 K. While for the Lu^{III} complex of DODPA the spectra are well-resolved at 298 K (Figure S1, Supporting Information), in the case of the Me-DODPA analogue the ^{1}H NMR spectrum recorded shows relatively broad signals for protons H8−H11. The proton spectrum of [Lu(DODPA)]$^+$ consists of 14 signals corresponding to 14 magnetically nonequivalent proton

dx.doi.org/10.1021/ic202436j | Inorg. Chem. 2012, 51, 2509−2521

environments in the ligand (see Scheme 1 for labeling), which points to an effective C_2 symmetry of the complex in solution. This is also confirmed by the ^{13}C NMR spectrum, which shows 11 peaks for the 22 carbon nuclei of the ligand backbone. The assignments of the proton signals (Table 4) were based upon

Table 4. ^1H and ^{13}C NMR Shifts for $[Lu(DODPA)]^+$ and Comparison of Experimental and Calculated ^1H Shifts for the $[Yb(Me\text{-}DODPA)]^+$ Complex at 278 K (pD ~ 7.0)[a]

		$[Yb(Me\text{-}DODPA)]^+$			
^1H	$[Lu(DODPA)]^+$[b]	δ_i^{exp}[c]	δ_i^{calc}[d]	^{13}C	$[Lu(DODPA)]^+$[b]
H3	7.96	−1.63	−7.19	C1	173.9
H4	8.20	−3.01	−3.36	C2	151.2
H5	7.80	−4.63	−2.73	C3	125.4
H7a	4.28	68.21	66.40	C4	144.3
H7b	4.72	−0.90	2.54	C5	128.2
H8ax	2.66	−71.42	−74.13	C6	158.7
H8eq	3.02	−20.59	−17.91	C7	63.0
H9ax	3.13	1.19	−0.60	C8	46.0
H9eq	2.68	−13.50	−12.13	C9	57.6
H10ax	3.31	87.45	86.14	C10	55.5
H10eq	3.11	25.25	28.22	C11	47.5
H11ax	3.27	16.98	17.59		
H11eq	2.99	26.90	23.95		

[a]See Scheme 1 for labeling. [b]Assignment supported by 2D COSY, HSQC and HMBC experiments at 298 K; $^3J_{3,4}$ = 7.7 Hz; $^3J_{5,4}$ = 7.9 Hz; $^2J_{7a,7b}$ = 16.2 Hz. [c]Assignment supported by 2D COSY experiments at 278 K. [d]Calculated values were obtained using eq 2 and the $\Lambda(\lambda\lambda\lambda\lambda)$ form of the complex optimized in aqueous solution at the mPWB95/6-31G(d) level.

HMQC and HMBC 2D heteronuclear experiments as well as standard 2D homonuclear COSY experiments, which gave strong cross-peaks between the geminal CH_2 protons (7−11) and between the ortho-coupled pyridyl protons. The ^1H NMR signal due to NH protons is observed at 4.04 ppm as a complicated multiplet due to coupling with protons H9 and H10. As previously observed for different metal complexes with secondary polyamines, the NH protons exchange very slowly with D_2O at about neutral pH.[45]

The signals due to protons H7a and H7b in $[Lu(DODPA)]^+$ show an AB pattern where the larger shift for H7b results from the combined deshielding effects of the pyridyl ring current and the polarizing effect of the Ln^{III} ion on the C−H bond pointing away from it.[46] It is known from previous ^1H NMR studies on Ln^{III} complexes with macrocyclic ligands that the ring axial protons experience strong coupling with the geminal protons and the vicinal axial protons, while the equatorial protons provide strong coupling with the geminal protons only.[47] Indeed, the $^3J_{H-H}$ coupling constants characterizing the coupling between vicinal pairs of protons (axial−axial, axial−equatorial and equatorial-equatorial) follow the Karplus equation [$^3J_{H-H} = 7 - \cos\phi + 5\cos 2\phi$, where ϕ represents the H−C−C−H dihedral angle and $^3J_{H-H}$ is given in Hz].[48] Thus, the specific assignment of the axial and equatorial protons could be achieved by observing the cross-peaks in the COSY spectra, as axial protons are expected to give two strong (geminal and axial−axial) and one weak (axial−equatorial) cross-peaks, whereas equatorial protons should show one strong (geminal) and two weak (equatorial-equatorial and equatorial-axial) cross-peaks.

The ^1H NMR spectra of paramagnetic $[Ln(Me\text{-}DODPA)]^+$ complexes (Ln = Eu or Yb) are well resolved (Figure 3, see also

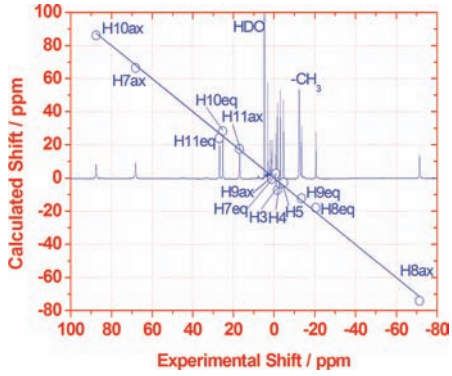

Figure 3. ^1H NMR spectrum of $[Yb(Me\text{-}DODPA)]^+$ recorded in D_2O solution (pD ~ 7.0) at 278 K and plot of experimental versus calculated shifts. The solid line represents a perfect fit between experimental and calculated values. See Scheme 1 for labeling.

Figure S2, Supporting Information). They consist of 13 signals corresponding to the 13 different proton magnetic environments of the ligand (see Scheme 1 for labeling), which points to effective C_2 symmetries of the complexes in solution, as observed previously for the $[Yb(BP12C4)]^+$ analogue.[16] The assignments of the proton signals in $[Yb(Me\text{-}DODPA)]^+$ (Table 4) were based on standard 2D homonuclear COSY experiments, which gave strong cross-peaks between the geminal CH_2 protons (7−11) and between ortho-coupled pyridyl protons. Additional cross-peaks between protons 8−9 and 10−11 allowed identifying the proton signals corresponding to each of the ethylenediamine units. The ten ^1H NMR peaks due to protons 7−11 can be grouped into two different sets according to their relative line broadening: five resonances with linewidths at half height of 135−200 Hz (at 500 MHz and 278 K), and five signals with linewidths in the range of 60−75 Hz (Figure 3). These two sets of signals correspond to two sets of Yb^{III}-proton distances, the broader resonances being associated with the protons closer to the metal ion.[49] Thus, the broader resonances were assigned to axial protons, while the second set of signals was assigned to equatorial ones.

To get more information on the solution structure of the Ln^{III} complexes of DODPA and Me-DODPA we have characterized the $[Ln(Me\text{-}DODPA)]^+$ systems (Ln = La, Nd, Eu, Gd, Ho, Yb, or Lu) by means of DFT calculations (mPWB95 model) performed in aqueous solution. On the basis of our previous experience,[50] the effective core potential (ECP) of Dolg et al.[32] and the related [5s4p3d]-GTO valence basis set were applied in these calculations. This ECP includes 46 + $4f^n$ electrons in the core, leaving the outermost 11 electrons to be treated explicitly. The use of large core ECPs has been justified by the fact that 4f orbitals do not significantly contribute to bonding because of their limited radial extension as compared to the 5d and 6s shells.[51]

The NMR spectra of the paramagnetic Eu^{III} and Yb^{III} complexes of Me-DODPA indicate that the complexes adopt a relatively rigid C_2 symmetry in solution (see above). As described previously for the BP12C4 complexes,[16] there are up to eight possible forms of the complexes (four enatiomeric pairs of diasteroisomers) consistent with a C_2 symmetry: $\Lambda(\lambda\lambda\lambda\lambda)$, $\Delta(\lambda\lambda\lambda\lambda)$, $\Lambda(\delta\lambda\delta\lambda)$, $\Lambda(\lambda\delta\lambda\delta)$ and their corresponding enantiomers $\Delta(\delta\delta\delta\delta)$, $\Lambda(\delta\delta\delta\delta)$, $\Delta(\lambda\delta\lambda\delta)$, $\Delta(\delta\lambda\delta\lambda)$. Our DFT

dx.doi.org/10.1021/ic202436j | Inorg. Chem. 2012, 51, 2509−2521

calculations provide the $\Lambda(\lambda\lambda\lambda\lambda)$, $\Delta(\lambda\lambda\lambda\lambda)$, $\Lambda(\lambda\delta\lambda\delta)$, and $\Lambda(\delta\lambda\delta\lambda)$ isomers as minimum energy conformations. The optimized geometries show slightly distorted C_2 symmetries (Figure 4), where the symmetry axis is perpendicular to the pseudoplane described by the four donor atoms of the crown moiety and contains the Ln^{III} ion. The relative energies of these isomers calculated for the $[Ln(Me\text{-}DODPA)]^+$ system are shown in Figure 5 and Table S1, Supporting Information.

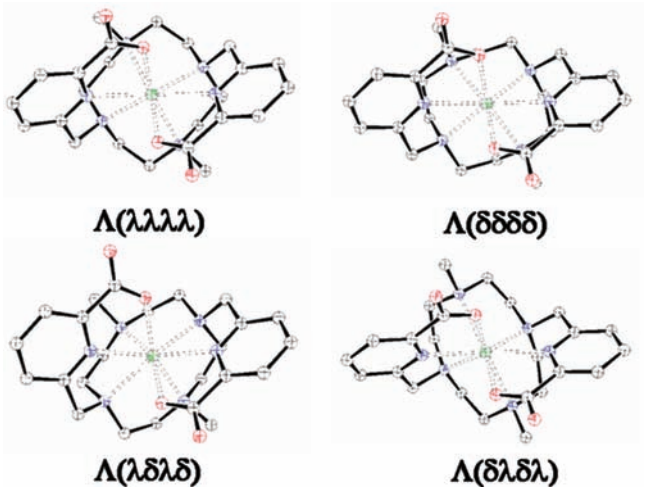

Figure 4. Geometries of $[Gd(Me\text{-}DODPA)]^+$ obtained from DFT calculations (mPWB95) in aqueous solution.

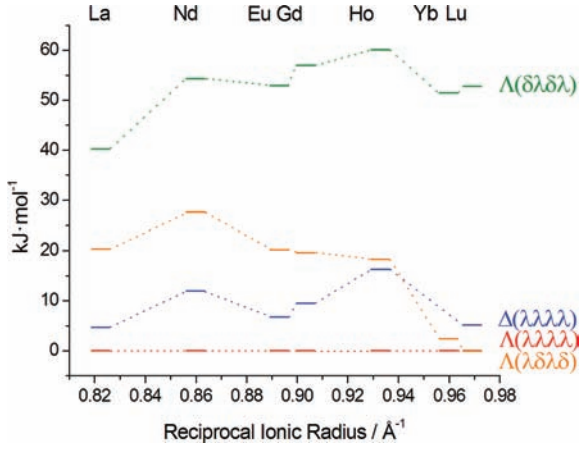

Figure 5. Relative free energies of the different diasterisomeric forms of $[Ln(Me\text{-}DODPA)]^+$ complexes obtained from DFT calculations in aqueous solution.

According to our calculations the $\Lambda(\lambda\lambda\lambda\lambda)$ isomer is the most stable one along the whole lanthanide series, with the exception of the Lu^{III} system, for which the $\Lambda(\lambda\delta\lambda\delta)$ form is more stable than the $\Lambda(\lambda\lambda\lambda\lambda)$ one by 0.10 kJ·mol^{-1}. These results suggest that the complexes may adopt a $\Lambda(\lambda\lambda\lambda\lambda)$ structure in solution.

Aiming to confirm the predictions of our DFT calculations we have analyzed the Yb^{III}-induced ^{1}H NMR shifts. Indeed, the binding of a ligand to a paramagnetic Ln^{III} ion such as Yb^{III} results in large NMR frequency shifts at the ligand nuclei, with magnitudes and signs depending on both the nature of the lanthanide ion and the location of the nucleus relative to the metal center.[52] Thus, the analysis of the NMR spectra of Ln^{III} paramagnetic complexes can provide useful structural information in solution. For a given nucleus i, the isotropic paramagnetic shift induced by a lanthanide ion j (δ_{ij}^{para}) is generally a combination of the Fermi contact (δ_{ij}^{con}) and dipolar (δ_{ij}^{dip}) contributions as given in eq 1, where the diamagnetic contribution δ_i^{dia} is obtained by measuring the chemical shifts for analogous diamagnetic complexes.

$$\delta_{ij}^{para} = \delta_{ij}^{exp} - \delta_i^{dia} = \delta_{ij}^{con} + \delta_{ij}^{dip} \quad (1)$$

The hyperfine ^{1}H NMR shifts in Yb^{III} complexes are considered to be largely pseudocontact in origin, and we therefore initiated the analysis of the paramagnetic shifts observed in the ^{1}H NMR spectrum of the Yb^{III} complex with the assumption that they are dominated by dipolar contributions, which can be written as linear combinations of the five components of the susceptibility tensor χ as given by the following equation:[53]

$$\delta_{ij}^{dip} = \left(\chi_{zz} - \frac{1}{3}Tr\chi\right)\left(\frac{3z^2 - r^2}{r^5}\right) + (\chi_{xx} - \chi_{yy})\left(\frac{x^2 - y^2}{r^5}\right) + \chi_{xy}\left(\frac{4xy}{r^5}\right) + \chi_{xz}\left(\frac{4xz}{r^5}\right) + \chi_{yz}\left(\frac{4yz}{r^5}\right) \quad (2)$$

With

$$r = \sqrt{x^2 + y^2 + z^2} \quad (3)$$

In eq 2 the Cartesian coordinates of atom i relative to the location of a paramagnetic ion are used in place of the more usual spherical coordinates. In the principal magnetic axis system $\chi_{xy} = \chi_{xz} = \chi_{yz} = 0$, and for axial symmetry $\chi_{xx} - \chi_{yy} = 0$. According to the Neumann's principle,[54] one of the principal magnetic axis of $[Yb(Me\text{-}DODPA)]^+$ must coincide with the 2-fold symmetry axis of the molecule. Thus, we assumed the z axis of the principal axis system of the magnetic susceptibility tensor coincides with the C_2 axis of the molecule. As a consequence, we only considered three (rather than five) parameters in the analysis of the paramagnetic shits, namely, the axial $[\chi_{zz} - 1/3(\chi_{xx} + \chi_{yy} + \chi_{zz})]$ and rhombic $(\chi_{xx} - \chi_{yy})$ anisotropies of the magnetic susceptibility tensor χ, and the orientation of the magnetic axis in the xy plane given by an angle α. The calculated DFT geometries of $[Yb(Me\text{-}DODPA)]^+$ in $\Lambda(\lambda\lambda\lambda\lambda)$, $\Delta(\lambda\lambda\lambda\lambda)$, $\Lambda(\delta\lambda\delta\lambda)$, and $\Lambda(\lambda\delta\lambda\delta)$ isomers were used to assess the agreement between the experimental and predicted Yb^{III}-induced paramagnetic shifts by using a least-squares fit relying on these three parameters. The ^{1}H NMR resonances due to protons of the macrocyclic fragment in $[Lu(Me\text{-}DODPA)]^+$ could not be assigned, as they are observed as broad signals due to exchange phenomena. For these proton nuclei the diamagnetic shift was estimated from those observed for $[Lu(DODPA)]^+$ (Table 4), while for the remaining proton nuclei the diamagnetic contribution was obtained from shifts observed for the Me-DODPA derivative [H3 8.05 ppm, H4 8.31 ppm, H5 7.92 ppm, H7ax 4.38 ppm and H7eq 4.83 ppm]. The DFT optimized structures of the $\Delta(\lambda\lambda\lambda\lambda)$, $\Lambda(\delta\lambda\delta\lambda)$ and $\Lambda(\lambda\delta\lambda\delta)$ isomers provided unacceptable agreements between the experimental and calculated Yb^{III}-induced shifts. On the contrary, the $\Lambda(\lambda\lambda\lambda\lambda)$ conformation provided an excellent agreement between experimental and calculated shifts (Figure 3) with $\chi_{zz} - 1/3(\chi_{xx} + \chi_{yy} + \chi_{zz}) = -113 \pm 40$ ppm·Å^3 and $\chi_{xx} - \chi_{yy} = 4628 \pm 67$ ppm·Å^3. Thus,

dx.doi.org/10.1021/ic202436j | Inorg. Chem. 2012, 51, 2509–2521

the analysis of the Yb^{III}-induced paramagnetic shifts unambiguously proves that this complex presents a $\Lambda(\lambda\lambda\lambda\lambda)$ [or $\Delta(\delta\delta\delta\delta)$] structure in aqueous solution, in agreement with the relative free energies reported in Figure 5, and the X-ray structure of $[Yb(DODPA)]^+$ (see above).

Once the structure in solution of the complexes was established, we used DFT calculations to investigate the reasons for the different hydration numbers determined for DODPA and Me-DODPA complexes from luminescence lifetime measurements. Thus, we performed full geometry optimizations of the $[Ln(DODPA)(H_2O)]^+$ and $[Ln(Me\text{-}DODPA)(H_2O)]^+$ systems. In these calculations only the $\Lambda(\lambda\lambda\lambda\lambda)$ isomer was considered. Figure 6 shows a plot of the

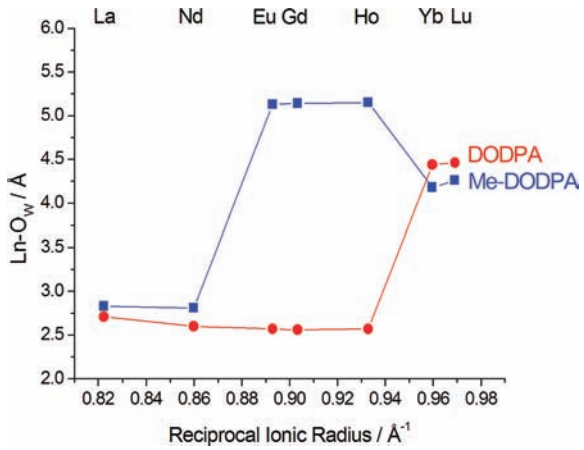

Figure 6. Distances between the Ln^{III} ion and the oxygen atom of the water molecule obtained from DFT calculations (aqueous solution) on the $[Ln(DODPA)(H_2O)]^+$ and $[Ln(Me\text{-}DODPA)(H_2O)]^+$ systems.

distances between the water molecule and the Ln^{III} ion for DODPA and Me-DODPA complexes. In the case of DODPA complexes the water molecule remains coordinated to the metal ion along the lanthanide series from La^{III} to Ho^{III}, and then it is expelled from the first coordination sphere for the smallest ions Yb^{III} and Lu^{III}. The corresponding optimized geometries show that in these cases the water molecule is hydrogen-bonded to the carboxylate groups of the ligand rather than coordinated to the metal ion (Figure S3, Supporting Information). This is in agreement with the X-ray structure of the Yb^{III} complex described above, which does not contain inner-sphere water molecules. In the case of Me-DODPA derivatives the water molecule remains coordinated to the metal ion only for the largest Ln(III) ions from La^{III} to Nd^{III}, and does not participate in metal ion coordination already around the middle of the lanthanide series for Eu^{III} and Gd^{III}. These results are in good agreement with the q values determined from luminescence lifetime measurements, and indicate an important degree of steric compression around the water binding site in Ln^{III}-DODPA complexes. The introduction of methyl groups increases this steric compression, which results in $q = 0$ complexes for at least the second half of the lanthandie series.

NMRD and ^{17}O NMR Studies. The relaxivity describes the efficiency of magnetic dipolar coupling occurring between water proton nuclei of the solvent and the paramagnetic metal ion (Gd^{III}), and represents a measure of the efficacy of a contrast agent in vitro. The relaxation rates of bulk water proton nuclei in the proximity of a gadolinium(III) ion are enhanced as a result of long- (outer-sphere relaxation) and short-range interactions (inner-sphere relaxation). Nuclear magnetic relaxation dispersion (NMRD) profiles of aqueous solutions of $[Gd(DODPA)]^+$ and $[Gd(Me\text{-}DODPA)]^+$ complexes were measured at 10, 25, and 37 °C in the proton Larmor frequency range 0.01−70 MHz, corresponding to magnetic field strengths varying between 2.343×10^{-4} and 1.645 T (Figure 7). Additionally, relaxivity of $[Gd(DODPA)]^+$

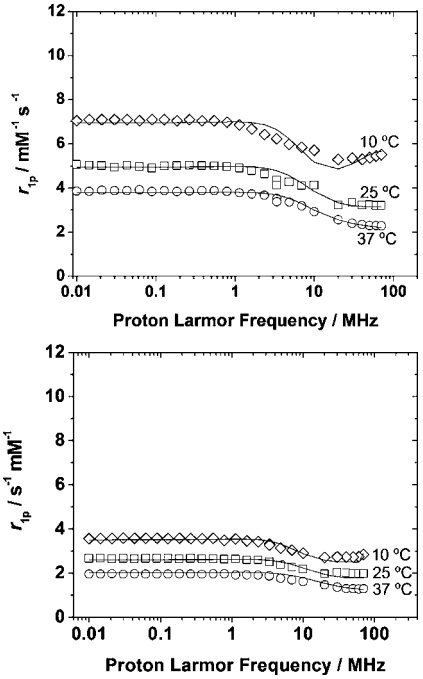

Figure 7. ^1H NMRD profiles of a $[Gd(DODPA)]^+$ (top) and $[Gd(Me\text{-}DODPA)]^+$ (bottom) recorded at different temperatures. The lines represent the fit of the data as explained in the text.

was investigated at 20 MHz in the temperature range 298−336 K (Figure 8). The NMRD profiles recorded for $[Gd(Me\text{-}DODPA)]^+$ are consistent with the absence of inner-sphere water molecules coordinated to the metal ion in this complex, the observed relaxivity being the result of the outer-sphere relaxation mechanism. By contrast, the relaxivities measured for the DODPA analogue are substantially higher, in line with the presence of both inner- and outer-sphere contributions. The relaxivity of $[Gd(DODPA)]^+$ decreases with increasing temperature; this shows that the relaxivity is limited by the fast rotation of the complex in solution, as usually observed for small Gd^{III} chelates.

As pointed out previously, it is difficult to determine the different parameters that determine the relaxivity of a given Gd^{III} complex without obtaining independent information for some of the most important parameters.[55] We therefore measured variable temperature ^{17}O NMR shifts and transversal relaxation rates in a 16 mM solution of the $[Gd(DODPA)]^+$ complex in H_2O (Figure 8) at neutral pH. The reduced transversal relaxation rates increase with decreasing temperature, which is characteristic of complexes endowed with a fast water exchange rate of the inner-sphere water molecule, the observed transversal relaxation rates being dominated by the relaxation rate of the bound water molecule.[15,17]

A simultaneous fitting of the NMRD and ^{17}O NMR data of $[Gd(DODPA)]^+$ was performed with the sets of equations given in the Supporting Information. The distance of closest

dx.doi.org/10.1021/ic202436j | Inorg. Chem. 2012, 51, 2509−2521

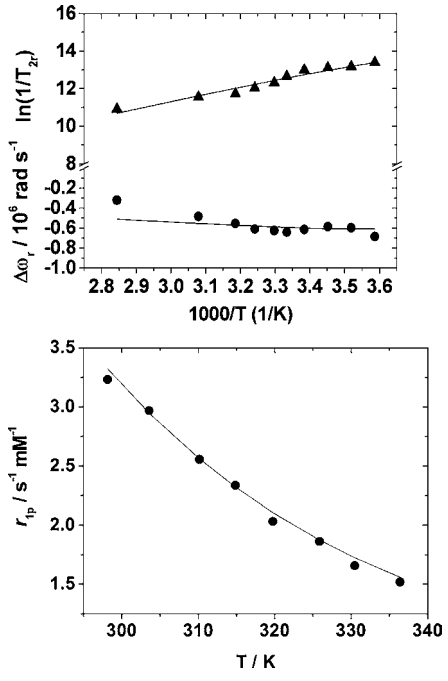

Figure 8. Top: Reduced transverse (▲) ^{17}O relaxation rates and ^{17}O chemical shifts (●) of a $[Gd(DODPA)]^+$ solution at 11.75 T and neutral pH; bottom: Temperature dependence of the ^1H relaxivity of $[Gd(DODPA)]^+$ at 0.47 T.

approach for the outer-sphere contribution a_{GdH} was fixed at 4 Å. The distance between the proton nuclei of the coordinated water molecule and the Gd^{III} ion (r_{GdH}) was fixed at 3.168 Å, which corresponds to the averaged distance obtained from DFT calculations (see above). The number of inner-sphere water molecules in the first coordination sphere was taken as 0.8, which corresponds to the average hydration number obtained from luminescence lifetime measurements for the Eu^{III} and Tb^{III} complexes. The parameters obtained from the fittings are listed in Table 5, while the curve fits are shown in Figures 7 and 8. The NMRD curves recorded for $[Gd(Me\text{-}DODPA)]^+$ were fitted according to the Freed equation for the outer-sphere contribution of the relaxivity, and the calculated parameters are also shown in Table 5. For comparison, previously reported data for $[Gd(DOTA)]^-$, $[Gd(DTPA)]^{2-}$, and $[Gd(BP12C4)]^+$ are also reported.

Inspection of the data reported in Table 5 reveals some similarities in the parameters that determine the relaxivity in the five complexes. The values obtained for the rotational correlation time (τ_R^{298}) of $[Gd(DTPA)]^{2-}$, $[Gd(DOTA)]^-$, and $[Gd(DODPA)]^+$ are very similar (58−77 ps). In the case of $[Gd(BP12C4)]^+$ the τ_R^{298} given in Table 5 was obtained from the analysis of longitudinal ^{17}O NMR relaxation rates, which are determined by dipole−dipole and quadrupolar relaxation, both related to rotation. Molecular dynamics and NMR investigations showed that the ratio of the rotational correlation time for the $Gd-H_{water}$ vector and that of the vector $Gd-O_{water}$ is about 0.75.[56] Thus, the τ_R^{298} value for the $Gd-H_{water}$ vector in $[Gd(BP12C4)]^+$ can be estimated to be ∼79 ps, in nice agreement with the values determined for the other systems given in Table 5.

The value obtained for the scalar coupling constant ($A/\hbar$) is smaller than those reported for other polyaminocarboxylate complexes with one inner-sphere water molecules (typically $(-3.6 \pm 0.3) \times 10^6$ rad s^{-1}).[1,54] The shift induced by a Gd^{III} complex to the water ^{17}O NMR resonance is proportional to q when the exchange between the coordinated water molecule and the bulk is fast on the NMR time-scale. Thus, the small value obtained for $A/\hbar$ could reflect a q value somewhat lower than 0.8, which corresponds to that obtained from luminescence lifetime measurements. However, relatively small values of $A/\hbar$ were previously obtained for other Gd^{III} complexes containing picolinate units,[57] which could be attributed to an efficient spin delocalization on the ligand backbone caused by the presence of aromatic units. The small value obtained for $A/\hbar$ could be also related to a long $Gd-O_{water}$ distance (2.56 Å according to our DFT calculations). The relatively high value of the activation energy for the relative diffusion coefficient obtained for $[Gd(DODPA)]^+$ (E_{DGdH} = 44.8 kJ·mol^{-1}), together with the low activation energy for the rotation (E_r = 8 kJ mol^{-1}) probably hide a certain dependence of q with temperature, as increasing temperature is expected to favor the species with the lowest hydration number.[58]

Given the traditionally used MRI field strengths in clinics (20−60 MHz), the typical simulated curves of proton relaxivities as a function of the exchange rate have usually been performed for 20 MHz, and the values cited as "optimal" exchange rate varied around $5-10 \times 10^7$ s^{-1}. At higher magnetic fields the ideal range of water exchange rates becomes much broader, so that the water exchange rate is not as critical

Table 5. Parameters Obtained from the Simultaneous Analysis of ^{17}O NMR and NMRD Data

parameter	$[Gd(DTPA)]^{2-}$ [a]	$[Gd(DOTA)]^-$ [a]	$[Gd(BP12C4)]^+$ [b]	$[Gd(DODPA)]^+$	$[Gd(Me\text{-}DODPA)]^+$
q^{298}	1.0	1.0	1.4	0.8[c]	0. 0[c]
$k_{ex}^{298}/10^6$ s^{-1}	3.3	4.1	220	58 ± 13	
$\Delta H^{\ddagger}$ kJ mol^{-1}	51.6	49.8	14.8	30.7 ± 3	
$A/\hbar/10^6$ rad s^{-1}	−3.8	−3.7	−3.4	−2.2 ± 0.2	
τ_R^{298}/ps	58	77	105	61.2 ± 4	
E_r/kJ mol^{-1}	17.3	16.1	15	8 ± 6	
τ_v^{298}/ps	25	11		15.0 ± 1.0	14.9 ± 1.6
$\Delta^2/10^{20}$ s^{-2}	0.46	0.16		1.0 ± 0.9	1.2 ± 0.2
E_v/kJ mol^{-1}	1.6	1.0		1.5 ± 1.2	
$D_{GdH}^{298}/10^{-10}$ m^2 s^{-1}	20	22		22.4	21.7 ± 0.7
E_{DGdH}/kJ mol^{-1}	19.4	20.2		44.8 ± 4	21.1 ± 0.7
r_{GdH}/Å	3.1	3.1		3.168[c]	
a_{GdH}/Å	3.5	3.5		4.0[c]	4.1

[a]Ref 55. [b]Ref 17. [c]Fixed in the fitting procedure.

dx.doi.org/10.1021/ic202436j | Inorg. Chem. 2012, 51, 2509−2521

to achieving high relaxivities.[59] The water exchange rate is very high on $[Gd(DODPA)]^+$, being at least 1 order of magnitude faster than for the $[Gd(DTPA)]^{2-}$, $[Gd(DOTA)]^-$ systems. In the case of $[Gd(DOTA)]^-$ the k_{ex}^{298} value reported in Table 5 corresponds to the averaged water exchange rate provided by the two isomers of the complex present in solution (actually two diasteroisomeric pairs of enantiomers), which are often denoted as square antiprismatic (SAP) and twisted square antiprismatic (TSAP). Different studies on DOTA derivatives have shown that the TSAP form presents a water exchange rate 1 order of magnitude faster than the SAP one,[60] which is attributed to the important degree of steric compression around the water binding site in the TSAP form.[61] In the case of $[Gd(DODPA)]^+$ the complex is present in solution exclusively as the $\Lambda(\lambda\lambda\lambda\lambda)$ [or $\Delta(\delta\delta\delta\delta)$] form, which provides a somewhat distorted TSAP coordination around the Ln^{III} ion (see above). This results in an important degree of steric compression around the bound water molecule, as confirmed by our DFT calculations described above, thereby resulting in a fast water exchange. However, the water exchange rate determined for $[Gd(DODPA)]^+$ is considerably slower than for $[Gd(BP12C4)]^+$ (ca. 3.7 times). We attribute the faster water exchange in $[Gd(BP12C4)]^+$ to an important degree of flexibility of the macrocyclic fragment in BP12C4 as compared to DODPA.

CONCLUSIONS

In this work we have presented two new octadentate ligands based on a cyclen platform that were designed for complexation of Ln^{III} ions in water. The ligands were prepared in good yields following two different procedures of selective *N*-protection: the preparation of the diBoc-cyclen, which leads to H_2DODPA, or the use of bisaminal chemistry, which gives its methylated analogue H_2Me-DODPA. A detailed investigation of the structure of the Ln^{III} complexes of Me-DODPA and DODPA shows that they exist in solution as the $\Lambda(\lambda\lambda\lambda\lambda)/\Delta(\delta\delta\delta\delta)$ enantiomeric pair, which provides a TSAP coordination around the Ln^{III} ion. The most striking result obtained in this study is the effect of introducing methyl groups in positions 4 and 7 of the cyclen unit on the hydration number of the complexes. Indeed, the $[Ln(DODPA)]^+$ complexes (Ln = Eu, Gd, or Tb) contain one inner-sphere water molecule, as demonstrated by the luminescence lifetime measurements on the Eu^{III} and Tb^{III} complexes, and the NMRD profiles recorded for the Gd^{III} analogue. However, the corresponding complexes of Me-DODPA do not contain inner-sphere water molecules. The inner-sphere water molecule in $[Gd(DODPA)(H_2O)]^+$ is endowed with a relatively fast water exchange rate, in line with an important degree of steric compression around the water binding site. The introduction of methyl groups increases this steric compression, which results in a $q = 0$ complex.

ASSOCIATED CONTENT

Supporting Information

HR-MS of DODPA and Me-DODPA complexes, ^{1}H NMR spectra of $[Eu(Me\text{-}DODPA)]^+$ and $[Lu(DODPA)]^+$ complexes, calculated relative energies of the different isomers of $[Ln(Me\text{-}DODPA)]^+$ complexes, optimized geometry of the $[Lu(DODPA)]^+\cdot H_2O$ system, optimized Cartesian coordinates (Å) of the complexes investigated in this work, and set of equations used for the fitting of the ^{17}O NMR and NMRD data. This material is available free of charge via the Internet at http://pubs.acs.org.

AUTHOR INFORMATION

Corresponding Author

*E-mail: ; Raphael.Tripier@univ-brest.fr (R.T.); carlos.platas.iglesias@udc.es (C.P.-I.).

ACKNOWLEDGMENTS

A.R.-R., D.E.-G., A. de B., T.R.-B., and C.P.-I. thank the Ministerio de Ciencia e Educación (MICINN, CTQ2009-10721), Fondo Europeo de Desarrollo Regional (FEDER, CTQ2009-10721) and Xunta de Galicia (IN845B-2010/063) for financial support. A.R.-R. thanks the Ministerio de Educación y Ciencia (FPU program) for a predoctoral fellowship, and the EU and University of Britanny for supporting short-term scientific missions to Alessandria (Italy) and Brest (France), respectively. M.F. and M.B thank support from Regione Piemonte (PIIMDMT Project). This research was performed in the framework of the EU COST Action D38 "Metal-Based Systems for Molecular Imaging Applications". The authors are indebted to Centro de Supercomputación de Galicia (CESGA) for providing the computer facilities.

REFERENCES

(1) *The Chemistry of Contrast Agents in Medical Magnetic Resonance Imaging*; Tóth, É., Merbach, A. E., Eds.; Wiley: New York, 2001.
(2) (a) Caravan, P.; Ellinson, J. J.; McMurry, T. J.; Lauffer, R. B. *Chem. Rev.* **1999**, *99*, 2293−2352. (b) Chan, K. W.-Y.; Wong, W.-T. *Coord. Chem. Rev.* **2007**, *251*, 2428−2451. (c) Terreno, E.; Delli Castelli, D.; Viale, A.; Aime, S. *Chem. Rev.* **2010**, *110*, 3019−3042.
(3) Mansson, S.; Bjornerud, A. Physical Principles of Medical Imaging by Nuclear Magnetic Resonance. In *The Chemistry of Contrast Agents in Medical Magnetic Resonante Imaging*; Tóth, E., Merbach, A. E., Eds.; Wiley: New York, 2001; pp 1−43.
(4) Pérez-Mayoral, E.; Negri, V.; Soler-Padrós, J.; Cerdán, S.; Ballesteros, P. *Eur. J. Radiol.* **2008**, *67*, 453−458.
(5) Cheng, S.; Abramova, L.; Saab, G.; Turabelidze, G.; Patel, P.; Arduino, M.; Hess, T.; Kallen, A.; Jhung, M. *JAMA* **2007**, *297*, 1542−1544.
(6) Brücher, E.; Sherry, A. D. Stability and Toxicity of Contrast Agents. In *The Chemistry of Contrast Agents in Medical Magnetic Resonante Imaging*; Tóth, E., Merbach, A. E., Eds.; Wiley: New York, 2001; pp 243−279.
(7) Frullano, L.; Caravan, P. *Curr. Org. Synth.* **2011**, *8*, 535−565.
(8) Caravan, P. *Acc. Chem. Res.* **2009**, *42*, 851−862.
(9) (a) De León Rodríguez, L. M.; Lubag, A. J. M.; Malloy, C. R.; Martinez, G. V.; Gillies, R. J.; Sherry, A. D. *Acc. Chem. Res.* **2009**, *42*, 948−957. (b) Mamedov, I.; Canals, S.; Henig, J.; Beyerlein, M.; Murayama, Y.; Mayer, H. A.; Logothetis, N. K.; Angelovski, G. *ACS Chem. Neurosci.* **2010**, *1*, 819−828. (c) Angelovski, G.; Mamedov, I. *Curr. Inorg. Chem.* **2011**, *1*, 76−90. (d) Geraldes, C. F. G. C.; Djanashvili, K.; Peters, J. A. *Future Med. Chem.* **2010**, *2*, 409−425.
(10) (a) Werner, E. J.; Datta, A.; Jocher, C. J.; Raymond, K. N. *Angew. Chem., Int. Ed.* **2008**, *47*, 8568−8580. (b) Aime, S.; Botta, M.; Terreno, E. *Adv. Inorg. Chem.* **2005**, *57*, 173−237.
(11) Jacques, V.; Dumas, S.; Sun, W.-C.; Troughton, J. S.; Greenfield, M. T.; Caravan, P. *Invest. Radiol.* **2010**, *45*, 613−624.
(12) Platas-Iglesias, C.; Mato-Iglesias, M.; Djanashvili, K.; Muller, R. N.; Vander Elst, L.; Peters, J. A.; de Blas, A.; Rodríguez-Blas, T. *Chem.—Eur. J.* **2004**, *10*, 3579−3590.
(13) Mato-Iglesias, M.; Platas-Iglesias, C.; Djanashvili, K.; Peters, J. A.; Tóth, É.; Balogh, E.; Muller, R. N.; van der Elst, L.; de Blas, A.; Rodríguez-Blas, T. *Chem. Commun.* **2005**, 47294731.
(14) Mato-Iglesias, M.; Balogh, E.; Platas-Iglesias, C.; Tóth, É.; de Blas, A.; Rodríguez-Blas, T. *Dalton Trans.* **2006**, 5404−5415.

(15) Balogh, E.; Mato-Iglesias, M.; Platas-Iglesias, C.; Tóth, É.; Djanashvili, K.; Peters, J. A.; de Blas, A.; Rodríguez-Blas, T. *Inorg. Chem.* **2006**, *45*, 8719−8728.
(16) Mato-Iglesias, M.; Roca-Sabio, A.; Pálinkás, Z.; Esteban-Gómez, D.; Platas-Iglesias, C.; Tóth, É.; de Blas, A.; Rodríguez-Blas, T. *Inorg. Chem.* **2008**, *47*, 7840−7851.
(17) Palinkas, Z.; Roca-Sabio, A.; Mato-Iglesias, M.; Esteban-Gómez, D.; Platas-Iglesias, C.; de Blas, A.; Rodríguez-Blas, T.; Tóth, E. *Inorg. Chem.* **2009**, *48*, 8878−8889.
(18) Hermann, P.; Kotek, J.; Kubicek, V.; Lukes, I. *Dalton Trans.* **2008**, 3027−3047.
(19) (a) Charbonnière, L.; Weibel, N.; Retailleau, P.; Ziessel, R. *Chem.—Eur. J.* **2007**, *13*, 346−358. (b) Charbonnière, L.; Mameri, S.; Kadjane, P.; Platas-Iglesias, C.; Ziessel, R. *Inorg. Chem.* **2008**, *47*, 3748−3762. (c) Regueiro-Figueroa, M.; Bensenane, B.; Ruscsak, E.; Esteban-Gómez, D.; Charbonniere, L. J.; Tircso, G.; Toth, I.; de Blas, A.; Rodríguez-Blas, T.; Platas-Iglesias, C. *Inorg. Chem.* **2011**, *50*, 4125−4141.
(20) (a) Nonat, A.; Gateau, C.; Fries, P. H.; Mazzanti, M. *Chem.—Eur. J.* **2006**, *12*, 7133−7150. (b) Nonat, A.; Fries, P. H.; Pecaut, J.; Mazzanti, M. *Chem.—Eur. J.* **2007**, *13*, 8489−8506. (c) Chatterton, N.; Gateau, C.; Mazzanti, M.; Pecaut, J.; Borel, A.; Helm, L.; Merbach, A. E. *Dalton Trans.* **2005**, 1129−1135. (d) Mameri, S.; Charbonnière, L.; Ziessel, R. *Tetrahedron Lett.* **2007**, *48*, 9132−9136. (e) Nonat, A.; Giraud, M.; Gateau, C.; Fries, P. H.; Helm, L.; Mazzanti, M. *Dalton Trans.* **2009**, 8033−8046.
(21) Corsi, D. M.; Platas-Iglesias, C.; van Bekkum, H.; Peters, J. A. *Magn. Reson. Chem.* **2001**, *39*, 723−726.
(22) *SABADS*, Version 2004/1; Bruker AXS Inc.: Madison, WI, 2004.
(23) *SHELX*; Sheldrick, G. M. *Acta Crystallogr.* **2008**, *A64*, 112−122.
(24) *WinGX* MS-Windows system of programs for solving, refining and analysing single crystal X-ray diffraction data for small molecules; Farrugia, L. J. *J. Appl. Crystallogr.* **1999**, *32*, 837−838.
(25) *DIRDIF2008*; Beurskens, P. T.; Beurskens, G.; de Gelder, R.; Garcia-Granda, S.; Gould, R. O.; Smits, J. M. M. Crystallography Laboratory, University of Nijmegen: Nijmegen, The Netherlands, 2008.
(26) De León-Rodríguez, L. M.; Kovacs, Z.; Esqueda-Oliva, A. C.; Miranda-Olvera, A. D. *Tetrahedron Lett.* **2006**, *47*, 6937−6940.
(27) Le Baccon, M.; Chuburu, F.; Toupet, L.; Handel, H.; Soibinet, M.; Déchamps-Olivier, I.; Barbier, J.-P.; Aplincourt, M. *New J. Chem.* **2001**, *25*, 1168−1174.
(28) Rohovec, J.; Gyepes, R.; Císarová, I.; Rudovsky, J.; Lukes, I. *Tetrahedron Lett.* **2000**, *41*, 1249−1253.
(29) Becke, A. D. *J. Chem. Phys.* **1996**, *104*, 1040−1046.
(30) Adamo, C.; Barone, V. *J. Chem. Phys.* **1998**, *108*, 664−675.
(31) Frisch, M. J.; Trucks, G. W.; Schlegel, H. B.; Scuseria, G. E.; Robb, M. A.; Cheeseman, J. R.; Scalmani, G.; Barone, V.; Mennucci, B.; Petersson, G. A.; Nakatsuji, H.; Caricato, M.; Li, X.; Hratchian, H. P.; Izmaylov, A. F.; Bloino, J.; Zheng, G.; Sonnenberg, J. L.; Hada, M.; Ehara, M.; Toyota, K.; Fukuda, R.; Hasegawa, J.; Ishida, M.; Nakajima, T.; Honda, Y.; Kitao, O.; Nakai, H.; Vreven, T.; Montgomery, Jr., J. A.; Peralta, J. E.; Ogliaro, F.; Bearpark, M.; Heyd, J. J.; Brothers, E.; Kudin, K. N.; Staroverov, V. N.; Kobayashi, R.; Normand, J.; Raghavachari, K.; Rendell, A.; Burant, J. C.; Iyengar, S. S.; Tomasi, J.; Cossi, M.; Rega, N.; Millam, N. J.; Klene, M.; Knox, J. E.; Cross, J. B.; Bakken, V.; Adamo, C.; Jaramillo, J.; Gomperts, R.; Stratmann, R. E.; Yazyev, O.; Austin, A. J.; Cammi, R.; Pomelli, C.; Ochterski, J. W.; Martin, R. L.; Morokuma, K.; Zakrzewski, V. G.; Voth, G. A.; Salvador, P.; Dannenberg, J. J.; Dapprich, S.; Daniels, A. D.; Farkas, Ö.; Foresman, J. B.; Ortiz, J. V.; Cioslowski, J.; Fox, D. J. *Gaussian 09*, Revision A.01; Gaussian, Inc.: Wallingford, CT, 2009.
(32) Dolg, M.; Stoll, H.; Savin, A.; Preuss, H. *Theor. Chim. Acta* **1989**, *75*, 173−194.
(33) Tomasi, J.; Mennucci, B.; Cammi, R. *Chem. Rev.* **2005**, *105*, 2999−3093.
(34) Develay, E.; Tripier, R.; Chuburu, F.; Le Baccon, M.; Handel, H. *Eur. J. Org. Chem.* **2003**, *16*, 3047−3050.
(35) Aime, S.; Barge, A.; Botta, M.; Fasano, M.; Ayala, J. D.; Bombieri, G. *Inorg. Chim. Acta* **1996**, *246*, 423−429.
(36) Bretonnière, Y.; Mazzanti, M.; Pècaut, J.; Dunand, F. A.; Merbach, A. E. *Inorg. Chem.* **2001**, *40*, 6737−6745.
(37) Aime, S.; Botta, M.; Fasano, M.; Marques, M. P. M; Geraldes, C. F. G. C.; Pubanz, D.; Merbach, A. E. *Inorg. Chem.* **1997**, *36*, 2059−2068.
(38) Corey, E. J.; Bailar, J. C. Jr. *J. Am. Chem. Soc.* **1959**, *81*, 2620−2629.
(39) Beattie, J. K. *Acc. Chem. Res.* **1971**, *4*, 253−259.
(40) Piguet, C.; Bünzli, J.-C. G.; Bernardinelli, G.; Bochet, C. G.; Froidevaux, P. *J. Chem. Soc., Dalton Trans.* **1995**, 83−97.
(41) Benetollo, F.; Bombieri, G.; Calabi, L.; Aime, S.; Botta, M. *Inorg. Chem.* **2003**, *42*, 148−157.
(42) Renaud, F.; Piguet, C.; Bernardelli, G.; Bünzli, J.-C. G.; Hopfgartner, G. *Chem.—Eur. J.* **1997**, *3*, 1646−1659.
(43) Supkowski, R. M.; Horrocks, W. D. Jr. *Inorg. Chim. Acta* **2002**, *340*, 44−48.
(44) Beeby, A.; Clarkson, I. M.; Dickins, R. S.; Faulkner, S.; Parker, D.; Royle, L.; de Sousa, A. S.; Williams, J. A. G.; Woods, M. *J. Chem. Soc., Perkin Trans. 2* **1999**, 493−503.
(45) (a) Liang, X.; Weishäupl, M.; Parkinson, J. A.; Parsons, S.; McGregor, P. A.; Sadler, P. J. *Chem.—Eur. J.* **2003**, *9*, 4709−4717. (b) Buckingham, D. A.; Clark, C. R.; Rogers, A. J. *J. Am. Chem. Soc.* **1997**, *119*, 4050−4058.
(46) Harris, R. K. *Nuclear Magnetic Resonance Spectroscopy: A Physicochemical view*; Pitman: London, U.K., 1983.
(47) Aime, S.; Botta, M.; Ermondi, G. *Inorg. Chem.* **1992**, *31*, 4291−4299.
(48) (a) Karplus, M. *J. Am. Chem. Soc.* **1963**, *85*, 2870−2871. (b) Geraldes, C. F. G. C.; Sherry, A. D.; Kiefer, G. E. *J. Magn. Reson.* **1992**, *97*, 290−304.
(49) Aime, S.; Barbero, L.; Botta, M.; Ermondi, G. *J. Chem. Soc., Dalton Trans.* **1992**, 225−228.
(50) Platas-Iglesias, C.; Roca-Sabio, A.; Regueiro-Figueroa, M.; Esteban-Gómez, D.; de Blas, A.; Rodríguez-Blas, T. *Current Inorg. Chem.* **2011**, *1*, 91−116.
(51) (a) Maron, L.; Eisenstein, O. *J. Phys. Chem. A* **2000**, *104*, 7140−7143. (b) Eisenstein, O.; Maron, L. *J. Organomet. Chem.* **2002**, *647*, 190−197.
(52) Peters, J. A.; Huskens, J.; Raber, D. J. *Prog. NMR Spectrosc.* **1996**, *28*, 283−350.
(53) Forsberg, J. H.; Delaney, R. M.; Zhao, Q.; Harakas, G.; Chandran, R. *Inorg. Chem.* **1995**, *34*, 3705−3715.
(54) Terazzi, E.; Rivera, J.-P.; Ouali, N.; Piguet, C. *Magn. Reson. Chem.* **2006**, *44*, 539−552.
(55) Powell, H. D.; Ni Dhubhghaill, O, M.; Pubanz, D.; Helm, L.; Lebedev, Y.; Schlaepfer, W.; Merbach, A. E. *J. Am. Chem. Soc.* **1996**, *118*, 9333.
(56) (a) Dunand, F. A.; Borel, A.; Merbach, A. E. *J. Am. Chem. Soc.* **2002**, *124*, 710−716. (b) Yerly, F.; Hardcastle, K. I.; Helm, L.; Aime, S.; Botta, M.; Merbach, A. E. *Chem.—Eur. J.* **2002**, *8*, 1031−1039.
(57) Platas-Iglesias, C.; Mato-Iglesias, M.; Djanashvili, K.; Muller, R. N.; Vander Elst, L.; Peters, J. A.; de Blas, A.; Rodríguez-Blas, T. *Chem.—Eur. J.* **2004**, *10*, 3579−3590.
(58) Graeppi, N.; Powell, D. H.; Laurenczy, G.; Zékány, L.; Merbach, A. E. *Inorg. Chim. Acta* **1995**, *235*, 311−326.
(59) Caravan, P.; Farrar, C. T.; Frullano, L.; Uppal, R. *Contrast Media Mol. Imaging* **2009**, *4*, 89−100.
(60) (a) Dunand, F. A.; Dickins, R. S.; Parker, D.; Merbach, A. E. *Chem.—Eur. J.* **2001**, *7*, 5160−5167. (b) Woods, M.; Aime, S.; Botta, M.; Howard, J. A. K.; Moloney, J. M.; Navet, M.; Parker, D.; Port, M.; Rousseaux, O. *J. Am. Chem. Soc.* **2000**, *122*, 9781−9792. (c) Aime, S.; Barge, A.; Botta, M.; De Sousa, A. S.; Parker, D. *Angew. Chem., Int. Ed.* **1998**, *37*, 2673−2675. (d) Woods, M.; Kovacs, Z.; Zhang, S.; Sherry, A. D. *Angew. Chem., Int. Ed.* **2003**, *42*, 5889−5892.
(61) (a) Parker, D.; Dickins, R.; Puschmann, H.; Crossland, C.; Howard, J. A. *Chem. Rev.* **2002**, *102*, 1977−2010. (b) Parker, D.;

Puschmann, H.; Batsanov, A. S.; Senanayake, K. *Inorg. Chem.* **2003**, *42*, 8646−8651.